Chaos

Synchronizability of directed networks: The power of non-existent ties

Cite as: Chaos **30**, 043102 (2020); https://doi.org/10.1063/1.5134920
Submitted: 03 November 2019 . Accepted: 16 March 2020 . Published Online: 01 April 2020

Kevin Daley, Kun Zhao, and Igor V. Belykh

Synchronizability of directed networks: The power of non-existent ties

Cite as: Chaos **30**, 043102 (2020); doi: 10.1063/1.5134920
Submitted: 3 November 2019 · Accepted: 16 March 2020 ·
Published Online: 1 April 2020

Kevin Daley,[1] Kun Zhao,[1,2] and Igor V. Belykh[1,3,a)]

AFFILIATIONS

[1]Department of Mathematics and Statistics, Georgia State University, 30 Pryor Street, Atlanta, Georgia 30303, USA
[2]Division of Viral Diseases, Centers for Disease Control and Prevention, 1600 Clifton Road NE, Mailstop H17-6, Atlanta, Georgia 30329, USA
[3]Lobachevsky State University of Nizhny Novgorod, 23 Gagarin Avenue, Nizhny Novgorod, 603950, Russia

Note: This paper is part of the Focus Issue on Symmetry and Optimization in the Synchronization and Collective Behavior of Complex Systems.

[a)]**Author to whom correspondence should be addressed:** ibelykh@gsu.edu

ABSTRACT

The understanding of how synchronization in directed networks is influenced by structural changes in network topology is far from complete. While the addition of an edge always promotes synchronization in a wide class of undirected networks, this addition may impede synchronization in directed networks. In this paper, we develop the augmented graph stability method, which allows for explicitly connecting the stability of synchronization to changes in network topology. The transformation of a directed network into a symmetrized-and-augmented undirected network is the central component of this new method. This transformation is executed by symmetrizing and weighting the underlying connection graph and adding new undirected edges with consideration made for the mean degree imbalance of each pair of nodes. These new edges represent "non-existent ties" in the original directed network and often control the location of critical nodes whose directed connections can be altered to manipulate the stability of synchronization in a desired way. In particular, we show that the addition of small-world shortcuts to directed networks, which makes "non-existent ties" disappear, can worsen the synchronizability, thereby revealing a destructive role of small-world connections in directed networks. An extension of our method may open the door to studying synchronization in directed multilayer networks, which cannot be effectively handled by the eigenvalue-based methods.

The power of weak ties in social networks[1] is a surprising principle, which indicates that the addition of your acquaintances (weak ties) to your network of friends (strong ties) can significantly enhance the transmission of novel information. This principle leverages the weak interpersonal ties in job hunting, match making, and growing a business. Similarly, the addition of possibly weak internodal ties typically favors synchronization in undirected dynamical networks via the small-world effect when additional shortcuts greatly facilitate information flows.[2] However, directed dynamical networks may have drastically different synchronization properties such that the addition of directed shortcuts may hamper synchronization. In this paper, we propose a general connection graph-based method, which helps explicitly assess how structural changes in directed networks influence synchronization. The method consists in symmetrizing the existing directed connections and augmenting the network with additional undirected links. These links can be viewed as "non-existent ties" between nodes that are not directly connected in the original directed network. We reveal the power of the "non-existent ties" in controlling synchronization in directed networks via structural changes of network topology. In particular, we demonstrate that the appearance of the "non-existent ties" as new edges in the augmented network due to the addition or removal of an edge in the directed network may offer a key to predicting a significant improvement or deterioration of the network synchronizability.

I. INTRODUCTION

Network synchronization is one of the most prevalent instances of cooperative behavior, manifesting itself in a wide spectrum of

real-world networks.[2–5] Examples include the disruption of neural synchrony causing cognitive dysfunction after traumatic brain injury,[6] synchronized neuronal firing during epileptic seizures and Parkinson's tremors,[7,8] synchronization of power generators for the operation of power-grid networks,[9] schooling fish moving as one large unit to confuse or escape from a predator,[10] and phase-locked gaits of pedestrians on a lively bridge.[11–13]

The interplay between network structure and individual node dynamics that controls the stability of synchronization has been extensively studied in oscillator networks,[14–36] including evolving[37–47] and multilayer networks.[48–52] This interplay yields a number of highly nontrivial, often counterintuitive effects. For example, it was shown that increasing heterogeneity of individual oscillators can enhance the stability of complete synchronization in networks of nonidentical oscillators.[53] Alternatively, the structural heterogeneity of a phase oscillator network can be modulated by heterogeneous natural oscillator frequencies to design synchrony-optimized networks.[36] In networks of bursting neurons with mixed coupling, (i) the addition of pairwise repulsive inhibitory connections to excitatory networks can promote synchronization[54] and (ii) combined electrical and inhibitory coupling can induce synchronization even though each coupling by itself promotes out-of-phase synchronization.[55] In multilayer networks, the surprising effects due to the multilayer structure include the "when good links go bad" phenomenon in which replacing a link by a pairwise stabilizing coupling via another layer can make the network unsynchronizable, turning the "good" link into a destabilizing connection.[52]

Complete synchronization in networks of continuous-time identical (or nearly identical) oscillators typically becomes locally or globally stable when the coupling strength exceeds a critical value.[17] The popular methods for determining the stability of complete synchronization as a function of network topology include the master stability function[14] and the connection graph method.[23] The master stability function is a semi-analytic local stability method that requires the calculation of two quantities: (i) the largest transversal Lyapunov exponent associated with the individual oscillator dynamics and (ii) the eigenvalues of the Laplacian connectivity matrix. The role of the network topology is, therefore, revealed via the dependence of the eigenvalues on the structure of a given oscillator network. The master stability function is generally applicable to any diagonalizable Laplacian matrix and, therefore, can handle both undirected and directed networks. In particular, it was applied to assess synchronization conditions in directed networks whose Laplacian connectivity matrices are asymmetric and typically have complex eigenvalues.[14] As a result, the stability conditions should take into account both real and imaginary parts of the eigenvalues.[56,57] While the calculation of the eigenvalues is fast and convenient, the mapping of structural network changes such as network rewiring or an edge addition, into the changes in the corresponding eigenvalues of the connectivity matrix is implicit in general. As a result, the direct impact of an edge addition or removal on the network synchronizability is difficult and often impossible to evaluate explicitly. The connection graph method[23] offers an alternate way to estimate the critical coupling required for the global stability of complete synchronization. This analytical method utilizes the Lyapunov function approach together with graph theoretical quantities expressed via the total lengths of chosen paths, which pass through a given edge. The method does not depend on explicit knowledge of the spectrum of the connectivity matrix, and, therefore, it provides a more explicit connection between structural network changes and the synchronization threshold. However, this method comes with the price of more conservative bounds and increased algebraic complexity of calculating the graph quantities. The extension of the connection graph method to directed networks, coined the generalized connection method,[24] consists in symmetrizing the directed graph and associating a weight to each edge and each chosen path. The synchronization condition for this symmetrized-and-weighted network then also guarantees synchronization in the original directed network.

Despite the availability of these powerful methods, the understanding of how synchronization in directed networks is influenced by structural changes in network topology is far from complete. For example, the addition of an edge in undirected Laplacian networks always increases the spectral gap defined by the second largest (least negative) eigenvalue of the Laplacian connectivity matrix and, therefore, lowers the synchronization coupling threshold in a wide class of oscillator networks, including coupled Lorenz oscillators.[23] At the same time, this addition may worsen synchronization in directed networks composed of the same oscillators. In particular, it was shown that strengthening or adding a directed connection may hinder synchronization in weakly connected networks composed of two strong components where one network component drives the other.[58] Based on a perturbation analysis of the spectral gap of the Laplacian matrix, this study focused on the impact of small structural perturbations of such two-component networks where a weak link is added to a network or the weight of an existing link is slightly perturbed.[58] However, the general problem of explicitly assessing the role of the addition or removal of potentially strong directed links to directed networks with arbitrary network topologies remained widely open.

In this paper, we seek to resolve this challenging problem by developing a general connection graph stability method that explicitly connects structural changes in network topology, such as the edge addition and removal as well as strengthening the existing connections, to the stability of complete synchronization in directed networks. Our general approach called the *augmented graph method* is an extension of the generalized connection graph method,[24] which is based on the transformation of a directed network into a symmetrized-and-weighted undirected network. The novel component of our augmented graph method is in augmenting the directed network by adding new undirected edges as a function of the pairwise mean degree imbalance of nodes, where the degree imbalance of a node is defined by the difference between its out- and in-degrees.[3] These augmenting edges can be viewed as "non-existent ties" in the original directed network and often control the location of critical nodes whose directed connections can be modified to improve or worsen the synchronizability of the network in a systematic way. In particular, applying our method to small-world directed networks, we demonstrate that the addition of long-range directed shortcuts, which changes the degree imbalance of the corresponding nodes and makes "non-existent ties" disappear, can worsen the synchronizability. Therefore, in contrast to the widely spread conception that small-world shortcuts generally facilitate cooperative properties of complex networks, our method reveals a potentially

destructive role of small-world connections when used in directed networks.

Our method originates from the connection graph method and, therefore, it yields bounds on the critical coupling strength, which depend on the choice of a path between any two nodes in the symmetrized-and-augmented network. The standard way of applying the connection graph method is to choose a shortest path between node i and node j and then identify the bottleneck edge with the maximum total length of the chosen paths. This bottleneck edge yields the bounds for synchronization in the entire network. However, often a different choice of paths can lead to lower bounds[27] such that optimizing the choice of paths allows one to lower the critical coupling bound when applying the augmented graph method. In this paper, we also develop an optimization algorithm, which assists the augmented graph method to deliver critical coupling bounds close to the actual ones obtained by the application of the eigenvalue-based methods.[14,21,22]

The layout of this paper is as follows. First, in Sec. II, we present the oscillator network model and state the problem under consideration. In Sec. III, we present the augmented graph method and formulate the main theorem that places upper bounds on the critical coupling strength, which guarantees global stability of synchronization in a directed network. In Sec. IV, we apply the method to specific directed networks and demonstrate that the addition of shortcut edges can destabilize synchronization. In Sec. V, we compare the synchronization bounds for directed networks of Lorenz oscillators obtained by the augmented graph method and the previous methods. In Sec. VI, a discussion of the obtained results is given. Finally, Appendix A contains the derivation of the augmented graph method. Appendix B presents the details of the optimization algorithm and gives an example of a network for which the optimization algorithm significantly lowers the synchronization bound. A Python code for the application of the augmented graph method to specific networks is available in a code repository.[59]

II. PROBLEM STATEMENT

We consider a directed network of n interacting oscillators described by the system

$$\frac{d\mathbf{x}_i}{dt} = \mathbf{F}(\mathbf{x}_i) + d\sum_{j=1}^{n} w_{ij} P \mathbf{x}_j, \quad i = 1, \ldots, n, \tag{1}$$

where $\mathbf{x}_i = (x_i^1, \ldots, x_i^h)$ is the h state vector containing the coordinates of the ith oscillator, the function $\mathbf{F} : \mathbb{R}^h \to \mathbb{R}^h$ determines the oscillators' individual dynamics. The oscillators are identical; however, the generalization of our results to non-identical oscillators with small parameter mismatch is straightforward.[23] P is an $h \times h$ projection matrix that selects the components of $\mathbf{x}_i$ which are involved in the interaction between the individual oscillators. Without loss of generality, we consider a vector version of the coupling with the diagonal matrix $P = \mathrm{diag}(p_1, p_2, \ldots, p_h)$, where $p_\nu = 1$, $\nu = 1, 2, \ldots, s$ and $p_\nu = 0$ for $\nu = s+1, \ldots, h$. The connection matrix D is an $n \times n$ asymmetrical Laplacian matrix with zero row-sums and nonnegative off-diagonal elements $d_{ij} = w_{ij} d$, yielding a directed connection graph $\mathbf{D}$. To facilitate the development and application of our method, the coupling strength dw_{ij} is introduced as a multiple of a uniform coupling constant d, where the weight w_{ij} can vary from one edge to another. The spectrum of the asymmetrical Laplacian connection matrix D contains possibly complex eigenvalues $\lambda_n \le \cdots \le \lambda_2 \le \lambda_1 = 0$ where the second largest eigenvalue $\lambda_2 < 0$ defines the spectral gap. In undirected networks, its absolute value is known as the algebraic connectivity.[60] This eigenvalue or its real part in the case of complex eigenvalues play an important role in determining the synchronizability of directed networks and will be used in the comparison analysis of Secs. IV and V.

In this paper, we develop the augmented graph method for assessing global stability of complete synchronization in which all oscillators of the network (1) acquire identical dynamical behavior such that $\lim_{t\to\infty} ||\mathbf{x}_i(t) - \mathbf{x}_j(t)|| = 0$ for $\forall i, j$ and any choice of initial conditions. Global stability of complete synchronization amounts to global stability of the synchronization manifold $S = \{\mathbf{x}_1(t) = \mathbf{x}_2(t) = \cdots = \mathbf{x}_n(t) = \mathbf{s}(t)\}$, where the synchronous solution $\mathbf{s}(t)$ is governed by the uncoupled individual oscillator.

Depending on the synchronization properties, oscillators composing network (1) can be formally divided into three main classes.[5] While there is no general convention upon labeling the corresponding classes and the labels are used interchangeably, we follow the classification[23,52] where Type I oscillators can synchronize and maintain stable synchronization for any coupling strengths exceeding a threshold value. This wide class of Type I oscillators includes Lorenz[61] and Chua[62] oscillators. A narrower Type II class of oscillators includes x-coupled Rössler systems[63] in which synchronization is stable within a bounded region of coupling parameter and looses its stability when the coupling becomes excessively strong.[14,15] Finally, Type III oscillators are unsynchronizable for any coupling strengths. Depending on what variables are used to couple the systems, some oscillators can change their synchronization properties and belong to each of the three types. For example, the one variable x, y, and z couplings between the tritrophic Rozenzweig–MacArthur prey–predator models[64] yield drastically different synchronization properties and places the oscillators in Type III, I, and II, respectively.[65] As only Type I oscillators are capable of synchronizing globally (from any initial conditions), in this paper, we limit our consideration to the large class of Type I oscillators.

We aim to predict when the synchronization manifold S is globally stable and explicitly connect its stability to the removal or addition of a directed link. Toward this goal, we develop the augmented graph method for deriving upper bounds on the coupling strength required to stabilize synchronization in oscillator networks with an arbitrary directed connection graph, under the constraint that the graph allows synchronization of all the nodes. It is important to emphasize that synchronization in directed networks is only possible if there is at least one node that directly or indirectly influences all the others.[20] In terms of the directed connection graph, this property requires the existence of a uniformly directed tree involving all the vertices. The simplest example of a directed network without such a tree is a three-node star network where two secondary nodes independently drive the hub, making synchronization impossible.

III. AUGMENTED GRAPH STABILITY METHOD

To derive our method and apply it to specific network topologies, we need to introduce and calculate important quantities.

Toward assessing the role of the individual oscillator and the choice of variables that couple the oscillators, we first need to prove that complete synchronization is globally stable in the simplest two-node directed network (1) with coupling strengths $d_{12} = w_{12}d$ and $d_{21} = 0$, provided that $d_{12} > a$, where a is a coupling threshold to be determined. In this setting, oscillator 1 is driven by oscillator 2 to globally stable synchronization, yielding a Type I oscillator network. Deriving a rigorous upper bound on the coupling threshold a is a fairly straightforward task that was previously performed for coupled Lorenz oscillators,[23] double-scroll Chua oscillators,[66] driven nonlinear pendulums,[67] tritrophic Rozenzweig–MacArthur prey-predator models,[65,68] Hindmarsh–Rose neuron oscillators,[27] and Hodgkin–Huxley-type neuron models.[55]

To formulate the main theorem that links the coupling threshold a for synchronization in the two-node network to the connection graph, we will transform the directed network (1) into a symmetrized-and-augmented undirected network. This is done by symmetrizing and weighting the underlying connection graph and adding new undirected edges, depending on the mean degree imbalance of each pair of nodes. The resulting undirected network typically has more edges than the original directed network and each undirected edge k connecting nodes i and j has coupling strength c_k, which depends on the in- and out-degrees of nodes i and j. We will then derive bounds on the coupling strengths c_k large enough to ensure stable synchronization in the symmetrized-and-augmented undirected network. The bound for each undirected edge k is calculated through the sum of the chosen path lengths between any two nodes i and j, which pass through edge k, where the path lengths are also weighted according to the in- and out-degrees of nodes i and j. These bounds on c_k are multiples of d and, therefore, yield the threshold value of d, which, in turn, guarantees stable synchronization in the original directed network (1) via $d_{ij} = w_{ij}d$.

The process of turning the directed network (1) into the symmetrized-and-augmented network and weighing the coupling strengths c_k and path lengths can be performed in the following steps.

Step 1. We calculate the degree imbalance for each node $D_i^b = \sum_{k\neq i}^{n}(w_{ki} - w_{ik})d$ as the difference between the sums of the coupling weights of all its outgoing edges (the out-degree of node i) and of all its incoming edges (the in-degree). Then, for each pair of nodes i and j, we calculate the mean degree imbalance $D_{ij}^b = \frac{D_i^b + D_j^b}{2}$.

Step 2. We symmetrize the directed connection graph $\mathbf{D}$ by replacing the edge directed from node i to node j by an undirected edge k with half the coupling strength coefficient $c_k^{sym} = w_{ij}d/2$. If there are two directed edges between nodes i and j: one from node i to node j and one in the reverse direction, the pair of directed edges should be replaced by an undirected edge k with mean coupling $c_k^{sym} = \frac{d_{ij}+d_{ji}}{2} = \frac{w_{ij}+w_{ji}}{2}d$. If the mean degree imbalance $D_{ij}^b < 0$ and there is an edge k connecting nodes i and j, we add an extra strength $\left|\frac{D_{ij}^b}{n}\right|$ to the mean coupling $c_k^{sym} = c_{ij}^{sym}$ of the symmetrized undirected edge. If the mean degree imbalance $D_{ij}^b < 0$ and there is no edge between nodes i and j, we create an undirected edge with coupling strength $c_k^{aug} = \left|\frac{D_{ij}^b}{n}\right|$, thereby augmenting the symmetrized connection graph to a total of m edges. As a result, edge k between nodes i and j on the symmetrized-and-augmented connection graph has the strength

$$
\begin{aligned}
c_k &= \begin{cases} c_k^{sym} \text{ for symmetrized edge } k \text{ with } D_{ij}^b \geq 0, \\ c_k^{sym} + c_k^{aug} \text{ for symmetrized } k \text{ with } D_{ij}^b < 0, \\ c_k^{aug} \text{ for augmenting edge } k, \text{ where} \end{cases} \\
c_k^{sym} &= \frac{w_{ij} + w_{ji}}{2}d \quad \text{and} \\
c_k^{aug} &= \left|\frac{D_{ij}^b}{n}\right| = \left|\frac{D_i^b + D_j^b}{2n}\right|, \quad \text{where} \\
D_i^b &= \sum_{l\neq i}^{n}(w_{li} - w_{il})d, \quad D_j^b = \sum_{l\neq i}^{n}(w_{lj} - w_{jl})d.
\end{aligned}
\tag{2}
$$

Thus, the edges of the symmetrized-and-augmented connection graph that correspond to the existing edges of the original directed graph have coupling c_k^{sym} or $c_k^{sym} + c_k^{aug}$, depending on the sign of the mean degree imbalance D_{ij}^b, whereas the new augmenting edges have weaker coupling c_k^{aug}. It is important to emphasize that these weaker connections do not exist in the original directed graph $\mathbf{D}$ and, therefore, represent "non-existent ties" between the corresponding nodes. However, these "non-existent ties" have the power to determine the synchronizability of the directed network $\mathbf{D}$, as will be shown later in the paper.

Step 3. We choose a path P_{ij} between each pair of nodes i and j, and determine its length $|P_{ij}|$ as the number of edges comprising the path. Usually, a shortest path should be chosen. However, optimizing the choice of paths, one may lower bounds on the critical coupling, especially in dense directed networks. This point will be discussed in more detail in Sec. V. If the mean degree imbalance D_{ij}^b is negative, then nodes i and j are always directly linked by either an augmenting edge or by a weighted combination of the augmenting edge and a symmetrized edge inherited from the original directed graph. Therefore, the corresponding length is $|P_{ij}| = 1$. To each of the other chosen paths between nodes i and j with $D_{ij}^b \geq 0$, we assign an extra weight $1 + \frac{D_{ij}^b}{a}$, thereby making its path length $(1 + \frac{D_{ij}^b}{a})P_{ij}$. Notice that if $D_{ij}^b = 0$, then the extra weight becomes zero. Therefore, the weighted length of the chosen path between any pair of nodes i and j is given by

$$
L(P_{ij}) = \begin{cases} |P_{ij}| = 1 & \text{if } D_{ij}^b < 0, \\ \left(1 + \frac{D_{ij}^b}{a}\right)P_{ij} & \text{otherwise.} \end{cases}
\tag{3}
$$

Step 4. Similarly to the generalized connection graph method,[24] we introduce a graph theoretical quantity b_k that characterizes the total length of the chosen weighted paths that go through each edge k on the symmetrized-and-augmented graph. In terms of traffic

networks, this quantity

$$b_k = \sum_{j>i;\ k\in P_{ij}}^{n} L(P_{ij}) \tag{4}$$

can be viewed as the total weighted length of the chosen roads that go through a given edge k which may be appropriately compared to a busy street. Therefore, we call b_k a "traffic" load on edge k.

Collecting the coupling threshold a for the simplest directed two-node network and the graph theoretical quantities identified in Steps 1–4, we place upper bounds on the coupling synchronization thresholds according to the following general theorem.

Theorem 1 (Augmented graph stability method). *Assume that the directed connection graph* **D** *has at least one node, which directly or indirectly drives all the others, thereby allowing complete synchronization in the n-node network (1). Then, globally stable complete synchronization in the directed network (1) with coupling weights $d_{ij} = w_{ij}d$ is guaranteed if the coupling constant d is large enough such that for each edge k of the symmetrized-and-augmented graph the following holds*:

$$c_k > \frac{a}{n} b_k, \quad k = 1, \ldots, m, \tag{5}$$

where the coupling strengths c_k are multiples of d and given in (2). The graph theoretical quantity b_k, which we colloquially refer to as a "traffic load" on edge k and defined in (4), represents the sum of the weighted path lengths $L(P_{ij})$ of all chosen paths P_{ij} which pass through a given edge k that belongs to the symmetrized-and-augmented graph. The weighted path length $L(P_{ij})$ is determined by the mean degree imbalance and defined in (3). The constant a is the coupling strength that is sufficient to ensure global stability of synchronization in the simplest two-node directed network (1) with $d_{12} = d$ and $d_{21} = 0$, thereby requiring the network to be of Type I. Therefore, the stability criterion (5) is restricted to Type I oscillator networks in which the synchronization emerges and remains stable for any coupling strength exceeding a threshold value.

Proof. The proof closely follows the steps of the derivation of the generalized connection graph method[24] for directed networks up to a point where the stability terms call for the introduction of augmenting edges which determine the concept of "non-existent ties" and play a pivotal role in understanding the synchronizability of directed networks. The complete proof is given in Appendix A. □

Remark 1. As the stability criterion (5) is formulated in terms of the symmetrized-and-augmented network, its practical application to the original directed graph might require an additional clarification. Recall that the coupling strengths of the directed edges are $d_{k_{ij}} = w_{ij}d$, where w_{ij} are given weights and d is the coupling to be varied to ensure stable synchronization. Thus, satisfying the criterion (5) for c_k yields the critical value of $d = d_k^*$ for each edge k of the symmetrized-and-augmented graph so that the maximum value $d^* = \max_k\{d_k^*\}$ should be substituted into $d_{k_{ij}} = w_{ij}d$ to obtain a distribution of coupling strengths d_{ij} that guarantees stable synchronization in the directed network. Often, the maximum value d^* corresponds to an augmenting edge that does not exist on the directed graph but controls synchronization in the entire directed network via this maximum value d^*, validating the power of the "non-existent ties."

Remark 2. The stability conditions (5) may yield conservative upper bounds on the coupling strengths sufficient for global stability of synchronization, and the eigenvalue-based methods yield a tighter, optimal bound. In terms of Theorem 1, this bound for directed networks with uniform coupling strengths $d_{ij} = d$ can be formulated for Type I oscillators as follows:[20,24] $d > a/|\Re\lambda_2|$, where $\Re\lambda_2$ is the real part of the second largest eigenvalue λ_2 of the Laplacian connection matrix D. However, the stability condition (5) allows for explicitly connecting changes in the network topology, including the removal and addition of links with the synchronizability of a given network. This task is often out of reach for the eigenvalue-based methods, as it is generally elusive to explicitly translate re-wiring or other structural changes in a directed network into an increase or decrease of $\Re\lambda_2$.

In Sec. IV, we will walk the reader through the application of the augmented graph stability method to specific directed networks and illustrate its predictive power.

IV. WHEN THE ADDITION OF EDGES DESTABILIZES SYNCHRONIZATION

To connect the general results to networks of specific Type I oscillators, hereafter, we will consider directed networks (1) of x-coupled Lorenz oscillators

$$\begin{aligned} \dot{x}_i &= \sigma(y_i - x_i) + \sum_{j=1}^{n} d_{ij}x_j, \\ \dot{y}_i &= rx_i - y_i - x_iz_i, \\ \dot{z}_i &= -bz_i + x_iy_i, \quad i = 1, \ldots, n, \end{aligned} \tag{6}$$

where σ, r, and b are intrinsic parameters. The coupling constant a used in the stability criterion (5) of Theorem 1 was previously calculated and explicitly expressed via the intrinsic parameters as follows:[23,69]

$$a = \frac{b(b+1)(r+\sigma)^2}{16(b-1)} - \sigma. \tag{7}$$

Derived through the application of a Lyapunov function, this completely rigorous bound is conservative. Alternatively, one could use a numerically assisted version of our method where a could be found numerically. In this semi-analytical setting, the constant a would play a role of the largest transversal Lyapunov exponent used in the master stability function.[14] For the standard parameters of the Lorenz system: $\sigma = 10$, $r = 28$, and $b = 8/3$, this numerically calculated constant $a \approx 7.79$.

Having estimated the impact of the individual oscillators comprising the directed network (1)–(6) in terms of constant a, we can apply the augmented graph method to specific networks, thereby revealing the role of the network topology and its structural changes.

A. A three-node network

Consider the three-node directed network (6) of Fig. 1(a) (top panel) with the coupling strengths $d_{21} = d$ and $d_{32} = 2d$. Below, we follow the four steps through which the augmented graph method can be applied to this network.

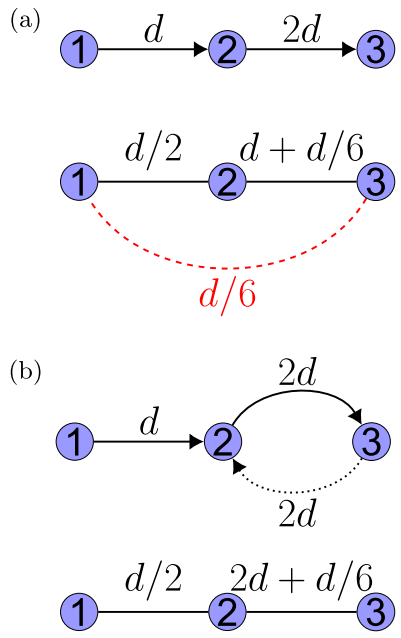

FIG. 1. Three-node network in which the addition of a strong reciprocal edge has a desynchronizing effect. (a) The original directed network (top panel) and its symmetrized-and-augmented counterpart (bottom panel). Notice the appearance of an augmenting edge (red dashed line) with coupling strength $d/6$, making the graph complete. (b) Network after the addition of a reciprocal edge (dotted gray arrowed line) (top panel). The corresponding symmetrized graph (bottom panel). Notice the absence of the augmenting edge, which makes the symmetrized network locally coupled. As predicted by the changes in the symmetrized-and-augmented network, the synchronizability of the directed network has worsened after the edge addition (also indicated by a drop in $|\lambda_2|$ from 1 to $|\frac{-5+\sqrt{17}}{2}| \approx 0.438$).

Step 1. The degree imbalance D_i^b for each node of the network is

$$D_1^b = d - 0 = d, \quad D_2^b = 2d - d = d, \quad D_3^b = 0 - 2d = -2d.$$

The mean degree imbalance $D_{ij}^b = \frac{D_i^b + D_j^b}{2}$ for each pair of nodes i and j is

$$D_{12}^b = d, \quad D_{23}^b = -\frac{d}{2}, \quad D_{13}^b = -\frac{d}{2}.$$

Step 2. Symmetrize the directed graph by replacing each directed edge by an undirected edge with half the coupling strength such that the strengths of the symmetrized edges are $c_{12}^{sym} = \frac{d}{2}$ and $c_{23}^{sym} = d$. Based on the mean degree imbalance D_{ij}^b identified in Step 1, (i) we add an extra coupling weight $|\frac{D_{ij}}{n}|$ to the existing edges of the symmetrized graph if $D_{ij}^b \le 0$; and (ii) we create an augmenting edge for each pair of nodes with $D_{ij} < 0$, which are not connected by a symmetrized edge. This results in creating the symmetrized-and-augmented graph depicted in Fig. 1(a) (bottom panel), where the coupling strengths are

$$c_{12} = c_{12}^{sym} = \frac{d}{2}, \quad c_{23} = c_{23}^{sym} + \left|\frac{D_{23}^b}{n}\right| = d + \frac{d}{6},$$
$$c_{13}^{aug} = \left|\frac{D_{13}}{n}\right| = \frac{d}{6}.$$

Notice that we have added weight $\frac{d}{6}$ to the existing edge between nodes 2 and 3 (edge e_{23}) because $D_{23}^b < 0$. We have also created an augmenting edge e_{13} with weight d_{13}^{aug} because $D_{13}^b < 0$ and the nodes 1 and 3 are not connected through the original directed graph.

Step 3. Choose the shortest path P_{ij} between nodes i, j of the symmetrized-and-augmented graph (there are three possible pairs of nodes) such that

$$P_{12} : e_{12}, \quad P_{23} : e_{23}, \quad P_{13} : e_{13}.$$

Since mean degree imbalances $D_{23}^b < 0$ and $D_{13}^b < 0$, the corresponding path lengths remain unweighted such that $L(P_{23}) = |P_{23}| = 1$ and $L(P_{13}) = |P_{13}| = 1$. As $D_{12}^b > 0$, we need to weigh $L(P_{12}) = 1 + \frac{d}{a}$.

Step 4. For each edge k of the symmetrized-and-augmented graph, calculate its traffic load b_k as the total length of the chosen weighted paths. In this particular example, the symmetrized-and-augmented graph is complete; therefore, there is only one chosen path comprised of one edge that goes through each of edges e_{12}, e_{23}, and e_{13}. Therefore,

$$b_{12} = L(P_{12}) = 1 + \frac{d}{a}, \quad b_{23} = L(P_{23}) = 1,$$
$$b_{13} = L(P_{13}) = 1.$$

Thus, the stability criterion (5) applied to the edges of the symmetrized-and-augmented graph of Fig. 1(a) (bottom panel) becomes

$$c_{12} = \frac{d}{2} > \frac{a}{3}\left(1 + \frac{d}{a}\right), \quad c_{23} = \frac{5d}{6} > \frac{a}{3}, \quad c_{13} = \frac{d}{6} > \frac{a}{3}. \tag{8}$$

The maximum value $d^* = 2a$ corresponds to the edge e_{12} and the augmenting edge e_{13} and yields an upper bound on the synchronization threshold in the symmetrized-and-augmented network. This bound in turn guarantees global stability of synchronization in the original directed network of Fig. 1(a) (top panel). In terms of the three-node directed network, this synchronization condition becomes

$$d_{21} > d^* = 2a, \quad d_{32} > 2d^* = 4a. \tag{9}$$

To study how structural changes in the three-node network affect synchronization, we add a reciprocal link between nodes 2 and 3, equal in weight to an existing directed link [see Fig. 1(b) (top panel)]. Intuitively, one could expect that the addition of this strong reciprocal edge, which makes the connection between nodes 2 and 3 undirected, should improve the synchronizability of the network. However, as the application of the augmented graph stability method (also verified through the calculation of $|\Re\lambda_2|$) indicates, this addition has the opposite, desynchronizing effect. The details are given below.

The addition of the reciprocal edge from node 3 to node 2 [Fig. 1(b) (top panel)] changes the degree imbalance of the nodes so that

$$D_1^b = d - 0 = d, \quad D_2^b = 0 - d = -d, \quad D_3^b = 2d - 2d = 0.$$

Therefore, it affects the mean degree imbalances so that

$$D_{12}^b = 0, \quad D_{23}^b = -\frac{d}{2}, \quad D_{13}^b = \frac{d}{2}.$$

As the mean degree imbalance D_{13}^b becomes positive, the augmenting link between nodes 1 and 3 is no longer present [cf. Fig. 1(a) (bottom panel)]. Therefore, the number of edges in the path P_{13} increases to 2 and this path becomes weighted by a factor of $(1 + \frac{d}{2a})$ due to $D_{13}^b > 0$. These changes also affect the weights of connections in the symmetrized-and-augmented network as depicted in Fig. 1(b) (bottom panel). Thus, the stability criterion (8) changes to

$$c_{12} = \frac{d}{2} > \frac{a}{3}\left(1 + 2 + \frac{d}{a}\right), \quad c_{23} = \frac{13d}{6} > \frac{a}{3}\left(1 + 2 + \frac{d}{a}\right).$$

These inequalities hold true when $d^* = 6a$ yielded by the maximum value c_{12}. Thus, the synchronization condition (8) for the network of Fig. 1(b) (bottom panel) after the addition of the reciprocal edge becomes

$$d_{21} > d^* = 6a, \quad d_{32} > 2d^* = 8a. \tag{10}$$

Notice the significant increase of the synchronization threshold bounds in the modified directed network predicted by the application of the augmented graph method. Alternatively, due to the small network size, the second largest eigenvalue λ_2 of both the original and modified networks can be computed analytically using the characteristic polynomials of the Laplacian matrices. It is $|\lambda_2| = 1$ for the original and $|\lambda_2| = \frac{-5+\sqrt{17}}{2} \approx -0.438$ for the modified network, thereby demonstrating that the addition of the directed strong edge hinders synchronization. This qualitatively agrees with the change in the bounds (8) and (10) computed by our method, but even in this simple three-node network, it is not immediately transparent from the characteristic polynomial what structural change in the network should lead to the desynchronization.

B. The destructive role of small-world shortcuts

The application of the augmented graph method to specific networks also reveals a surprising role of directed small-world shortcuts in reducing the synchronizability of directed networks. The directed networks of Figs. 2 and 3 are examples which illustrate this claim.

Similarly to the example of Fig. 1, we first consider the five-node network depicted in Fig. 2(a) (left), together with its structural modification with two added shortcut edges [Fig. 2(b) (left)]. We first apply our method to the unmodified, locally coupled network of Fig. 2(a) (left) with the coupling weights $d_{21} = 7d/10$, $d_{32} = 14d/5$, $d_{43} = 10d$, and $d_{14} = 10d$. As before, we should follow the four steps of the method.

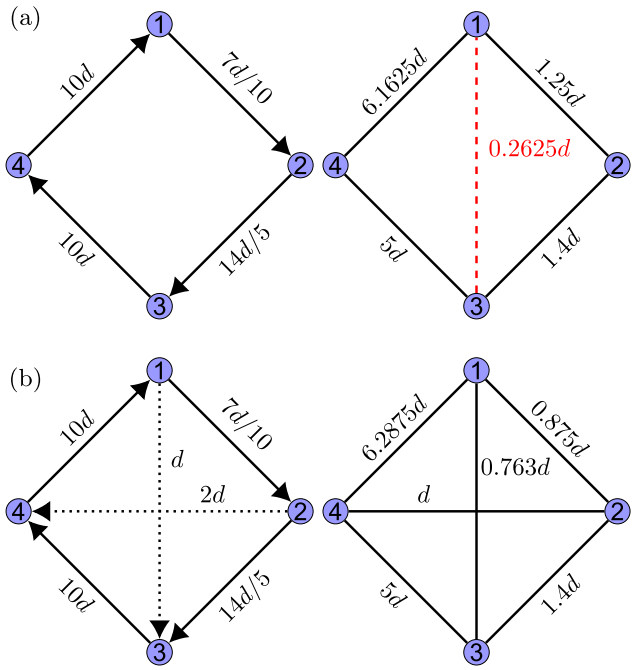

FIG. 2. Four-node network in which the addition of two shortcut edges hinders synchronization. (a) Locally coupled directed network before modification (left); the corresponding symmetrized-and-augmented graph with one augmenting edge (red dashed edge) (right). (b) Network after the addition of two strong shortcut edges (dotted arrowed edges) (left); its symmetrized analog without augmenting edges (right). Remarkably, the symmetrized network becomes fully connected, but the synchronizability of the directed network with the two added shortcuts worsens as predicted by the augmented stability method and verified through the decrease of $|\lambda_2|$ from 4.5061 to 3.3727 due to the change in the mean degree imbalance.

Step 1. The degree imbalance of each node is

$$D_1^b = 0.7d - 10d = -9.3d, \quad D_2^b = 2.8d - 0.7d = 2.1d,$$
$$D_3^b = 10d - 2.8d = 7.2d, \quad D_4^b = 10d - 10d = 0.$$

The mean degree imbalance $D_{ij}^b = \frac{D_i^b + D_j^b}{2}$ for each pair of nodes is then

$$D_{12}^b = -3.6d, \quad D_{13}^b = -1.05d, \quad D_{14}^b = -4.65d,$$
$$D_{23}^b = 4.65d, \quad D_{24}^b = 1.05d, \quad D_{34}^b = 3.6d.$$

Step 2. Exactly as in the three-node example of Fig. 1, we symmetrize and augment the graph and strengthen edges with negative degree imbalance; the resultant undirected network is depicted in Fig. 2(a) (right). Here, we have augmented the network with an edge e_{13} of strength $c_{13} = 1.05d/4 = 0.2625d$. The strengths of the symmetrized edges e_{12}, e_{23}, e_{34}, and e_{14} inherited from the directed network are $c_{12} = 1.25d$, $c_{23} = 1.4d$, $c_{34} = 5d$, and $e_{14} = 6.1625d$, respectively.

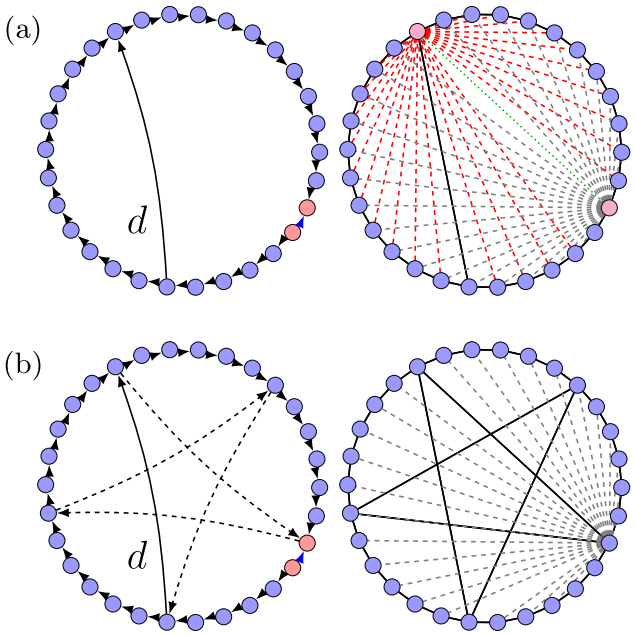

FIG. 3. Small-world network in which the addition of four directed shortcuts significantly worsens its synchronizability. (a) The original network (left): a directed ring of 30 nodes with a single reversed directed edge (between the two orange nodes) and one shortcut edge. The coupling strength d is uniform for all edges. The symmetrized-and-augmented graph (right): there are, in total, 51 augmenting edges; one with weight $d/20$ (green dotted line between the magenta nodes), 25 edges with weight $d/30$ (gray dashed lines), and 25 edges having weight $d/60$ (red dashed lines). The actual synchronization threshold is determined by $\frac{a}{|\Re\lambda_2|} = a$. (b) The modified network upon the addition of four shortcuts (dashed lines) with uniform coupling strength d (left). The symmetrized-and-augmented graph (right): the number of augmenting edges has reduced significantly; the 25 gray edges from the unperturbed symmetrized-and-augmented graph in (a) remain, while all other augmenting edges have disappeared. The synchronization threshold increases by more than an order of magnitude, to $\frac{a}{|\Re\lambda_2|} = 15.1515a$.

Step 3. As in the previous example, we select the shortest paths between endpoints of each node pair in the symmetrized-and-augmented graph of Fig. 2(a) (right),

$$\begin{aligned} &P_{12}: e_{12}, \quad P_{13}: e_{13}, \quad P_{14}: e_{14}, \\ &P_{23}: e_{23}, \quad P_{24}: e_{12}, e_{14}, \quad P_{34}: e_{34}, \end{aligned}$$

where the lengths of the following paths must be weighted as their endpoint nodes have a negative mean degree imbalance D_{ij}^b

$$L(P_{23}) = 1 + \frac{2.325d}{a}, \quad L(P_{24}) = 2 + \frac{1.05d}{a},$$
$$L(P_{34}) = 1 + \frac{1.8d}{a}.$$

Step 4. Calculating the traffic load b_k for each edge e_{12}, e_{23}, e_{34}, e_{14} of the symmetrized-and-augmented graph and collecting the weighted coupling strengths, we can write the stability criterion (5) for the edges of the symmetrized-and-augmented graph

$$c_{12} = 1.25d > \frac{a}{4}\left(3 + \frac{1.05d}{2a}\right), \quad c_{13} = 0.2625d > \frac{a}{4},$$
$$c_{23} = 1.4d > \frac{a}{4}\left(1 + \frac{2.325d}{a}\right), \quad c_{34} = 5d > \frac{a}{4}\left(1 + \frac{1.8d}{a}\right),$$
$$c_{14} = 6.1625d > \tfrac{a}{4}\left(3 + \frac{1.05d}{2a}\right).$$

This stability criterion is constrained by the inequality on the bottleneck edge e_{23} yielding the bound $d^* = 0.91a$. Therefore, this bound determines the stability criterion for the directed network of Fig. 2(a) (left)

$$\begin{aligned} &d_{21} > 7d^*/10 = 0.637a, \quad d_{32} > 14d^*/5 = 2.548, \\ &d_{43} > 10d^* = 9.1a, \quad d_{14} > 10d^* = 9.1a. \end{aligned} \tag{11}$$

To better illustrate that the addition of small-world shortcuts, which improves the connectivity of a directed network, may reduce its synchronizability, we modify the *locally* coupled network Fig. 2(a) (left) in an extreme way by adding two shortcuts [Fig. 2(b) (left)]. According to our method, this modification yields a *globally* coupled symmetrized network of Fig. 2(b) (right), which has no augmenting edges. Let us check how this modification affects the stability criterion (11).

The addition of shortcut edges with coupling weights $d_{31} = d$ and $d_{42} = 2d$ changes the degree imbalance of each node:

$$D_1^b = -10.3d, \quad D_2^b = 4.1d, \quad D_3^b = 6.2d, \quad D_4^b = -2d$$

so that the mean degree imbalances associated with each pair become

$$\begin{aligned} &D_{12}^b = -3.1d, \quad D_{13}^b = -2.05d, \quad D_{14}^b = -6.15d, \\ &D_{23}^b = 5.15d, \quad D_{24}^b = 1.05d, \quad D_{34}^b = 2.1d. \end{aligned}$$

Remarkably, the primary effect of making the symmetrized graph fully connected is essentially in increasing the degree imbalance of nodes 2 and 3, connected by edge e_{23}, which is the bottleneck edge of the unperturbed network without the shortcuts. As in the previous example, it is straightforward to show that this edge is also the bottleneck of the fully connected symmetrized network. As a result, the modified inequality $c_{23} = 1.4d > \frac{a}{4}(1 + \frac{5.15d}{a})$ yields the bound $d^* > 6.667a$. Thus, the addition of the two small-world shortcuts increases the synchronization criterion bound from $d^* = 0.91a$ to $d^* = 6.667a$, suggesting that the perturbed network becomes more resistant to synchronization. Based on the Lyapunov functions used to prove global stability of synchronization, our method gives sufficient stability conditions in the form of upper bounds d^*. Therefore, the magnitude of the predicted change in the synchronization stability criterion differs from the actual one estimated by numerically calculated $|\lambda_2|$, which decreased from 4.5061 to 3.3727 upon the addition of the two shortcuts.

To convince the reader that the desynchronizing effect of small-world connections is also present in larger directed networks, we consider an unweighted directed ring of 30 oscillators with a single reversed directed edge [Fig. 3(a)] and then modify this network by adding four extra shortcut edges in a five-point star configuration with the existing shortcut [Fig. 3(b)]. Applying our method to the

unperturbed network of Fig. 3(a) (left), we obtain the symmetrized-and-augmented network of Fig. 3(a) (right), which contains 51 weighted augmenting edges. Remarkably, the addition of the four small-world shortcuts significantly reduces the number of augmenting edges in the corresponding symmetrized-and-augmented network of Fig. 3(b) (right). More precisely, this addition preserves only 25 augmenting edges with weight $d/20$, making the other 26 augmenting edges disappear; instead, it only offers four symmetrized connections corresponding to the four directed shortcuts. As the augmenting edges help decrease the traffic load on the edges existing in the original directed network by offering detours around the heavily loaded bottleneck edges, it is natural to hypothesize that the disappearance of nearly a half of these augmenting shortcuts should significantly worsen the synchronizability of the perturbed network. This straightforward conclusion does offer a correct, qualitative prediction, which leverages the predictive power of the "non-existent ties" (augmenting edges) even without going into the detailed calculations of the upper bounds through the stability criterion (5). We knowingly omit these calculations and test this claim directly through changes in the actual synchronization threshold $a/|\Re\lambda_2|$ which, as predicted by the disappearance of 26 out of 51 augmenting edges, indicates a sharp increase by more than an order of magnitude, from a to $15.15a$ upon the addition of the four small-world shortcuts.

As in the previous examples, predicting this sharp change in terms of a potential impact of the shortcut addition on the eigenvalue λ_2—without actually calculating it—represents a significant challenge and seems elusive. In light of this, the appearance or disappearance of a large portion of "non-existent ties" might be used as a simple indicator of a significant improvement or deterioration of the network synchronizability.

V. COMPARISON WITH THE EXISTING METHODS

In order to compare the proposed augmented graph method with the existing generalized connection graph method[24] and the eigenvalue-based methods,[14,21,22] we consider two more networks of coupled Lorenz oscillators (1)–(6) for which the numerically calculated constant $a = 7.79$ is chosen instead of the more conservative analytical bound (7).

The first example (depicted in Fig. 4) is a 62-node network of two identical undirected components with their hubs connected by an asymmetrical coupling. The asymmetry introduced via parameter ω induces 30 augmenting edges of strength $\frac{\omega-1}{124}$ in the symmetrized-and-augmented graph [Fig. 4(a) (bottom)]. As a result, increasing ω lowers the actual synchronization threshold ($d^* = a/|\Re\lambda_2|$) and its bounds due to the augmented graph and generalized connection graph methods. The generalized connection graph, which consists in symmetrizing directed connections, outperforms the augmented graph method when the asymmetry is fairly small ($\omega < 2$). In this case, the contribution of weak augmenting edges is less significant than an additional strengthening of the existing connections due to the generalized connection method. However, the proposed augmented graph method yields significantly lower bounds in the stronger asymmetrical network ($\omega > 2$), which approach the optimal bounds due to the eigenvalue method. It is worth noticing that increasing the asymmetry of the directed connection which makes one component a stronger driver of the other consistently improves the synchronizability. This observation agrees with the previous study of networks, which are composed of two strongly connected components and coupled via a weak directed link whose strengthening can improve synchronization.[58]

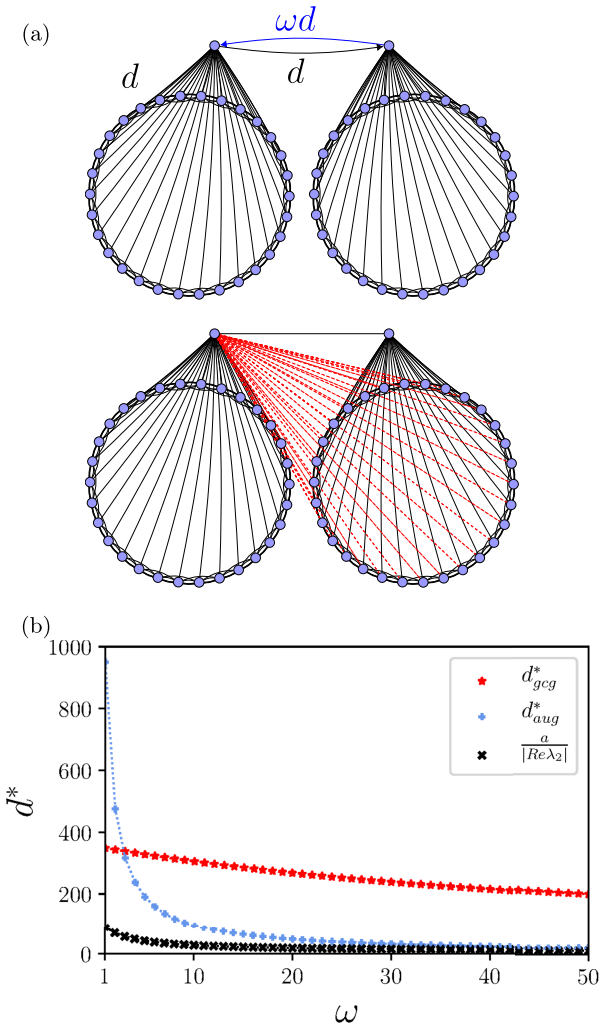

FIG. 4. (a) Network of two identical undirected components asymmetrically coupled via their hubs. Each component is a four-nearest-neighbor ring of 30 nodes with undirected connections to a hub. The coupling within each component has uniform strength d. Asymmetrical connections between the hubs have strengths d and ωd (top). Corresponding symmetrized-and-augmented network with augmenting edges (red dashed lines) all of strength $\frac{\omega-1}{124}$ (bottom). (b) Bound on the synchronization threshold d^* in the asymmetrical network as a function of parameter ω, calculated by the augmented graph method (d^*_{aug}, blue markers), the generalized connection graph method[24] (d^*_{gcg}, red markers), and the eigenvalue method ($d^* = a/|\Re\lambda_2|$, black markers). Constant $a = 7.79$ relates to networks of x-coupled Lorenz oscillators (6). The augmented graph method yields significantly lower bounds compared to the generalized connection graph method (for $\omega > 2$) and approaches the performance of the eigenvalue method when the asymmetry increases via ω.

To further investigate how the relative performance of the methods changes when network connectivity increases, we consider the network of Fig. 5. This is a $2K$-nearest-neighbor network with additional outbound connections from one node to all other nodes. The application of the augmented graph method to this network yields a symmetrized-and-augmented graph, which has augmenting edges of weight $\frac{d}{50}$ between every node pair except for those containing the source node (not shown). As a result, the augmented method performs better than the generalized connection graph in sparser networks with lower K [see Fig. 5 (bottom)] due to the stronger impact of the added augmented edges. As the local connectivity of the network increases with K, it approaches a complete network and the generalized connection graph method becomes more viable. Notably, increasing K by one corresponds to the addition of two reciprocal edges to the outbound edges from the source node, reducing the degree imbalance of two nodes to zero. In terms of the symmetrized-and-augmented graph, this reduces the number of augmenting edges and worsens the relative performance of the augmented graph method as K increases.

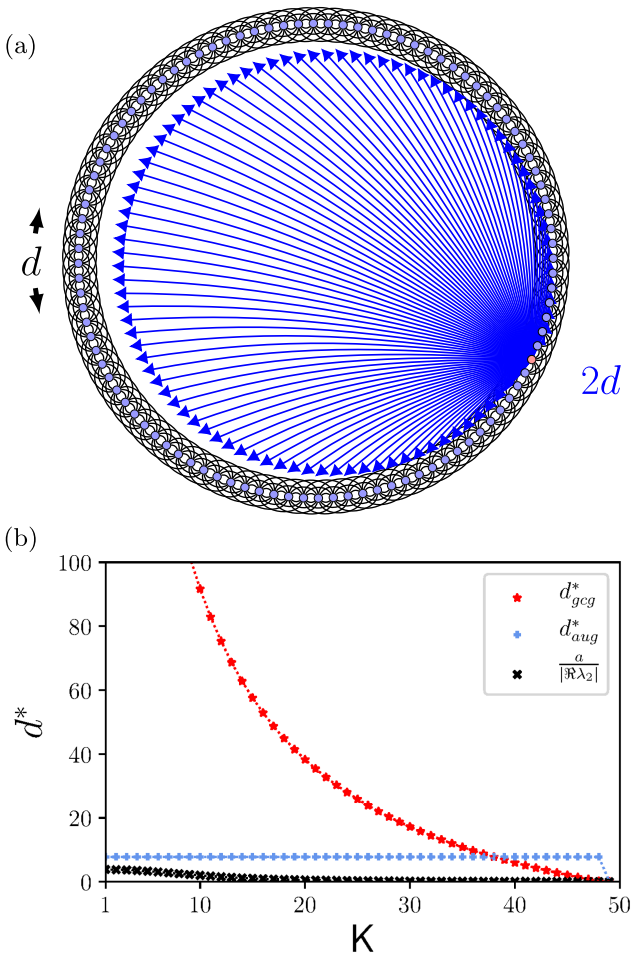

FIG. 5. (a) $2K$-nearest-neighbor ring of 100 nodes with additional directed connections (blue arrowed lines) from one source node (pink). Undirected local connections within the ring and directed shortcuts have strengths d and $2d$, respectively. (b) Bound on the synchronization threshold d^* as a function of K, calculated by the augmented graph method (d^*_{aug}), generalized connection graph method (d^*_{gcg}), and the eigenvalue method. Constant $a = 7.79$ as in Fig. 4. The augmented graph method performs significantly better than the generalized connection method and closer to the eigenvalue method in sparser networks (with lower K).

In the above examples, we have chosen shortest paths to derive the synchronization bounds (5). While this choice is convenient and often unique in a sparse network, it often leads to the appearance of bottleneck edges with a high traffic load b_k, which makes the synchronization bound conservative. In light of this, the performance of the augmented graph method can be improved by optimizing the choice paths between two nodes through a simple algebraic rearrangement. This is particularly relevant to dense networks, which offer a rich choice of possible paths between nodes. We have developed such an optimization algorithm that reroutes certain paths through "high-traffic" edges and, therefore, lowers the synchronization bound (5) for the bottleneck edge by increasing synchronization bounds for other less loaded edges of the symmetrized-and-augmented graph. This algorithm is described in Appendix B through an example of the network depicted in Fig. 6. Its Python implementation is available online.[59]

VI. CONCLUSIONS

The synchronizability of directed oscillator networks with diffusive coupling is known to be controlled by the eigenvalues of the Laplacian connection matrix. However, the general problem of explicitly assessing how a structural modification of the directed network topology (for example, the addition, removal, or re-weighting of an edge) changes the spectrum of the connectivity matrix is far from being solved. Therefore, it is often difficult to predict significant changes in the synchronizability of a directed network caused by local modifications of its structure, unless a specific class of weakly coupled directed networks and small structural perturbations are considered.[58]

In this paper, we sought to close this gap by creating a novel connection graph stability method, which links the synchronizability of a directed network with its possible structural modifications without relying on the spectrum of the Laplacian connection matrix. This augmented graph method for determining global stability of synchronization in a directed network combines the Lyapunov function method with graph theoretical quantities such as the degree imbalance of a node and a traffic load on an edge. Drawing parallels to traffic on busy streets, we defined the traffic load on an edge as the total weighted length of the chosen paths that pass through the edge. The principal novel component of the method is in symmetrizing and augmenting the directed graph and analyzing the non-local effects of the mean degree imbalance among nodes that control the appearance of augmenting edges. Remarkably, the emergence or disappearance of the augmenting edges (termed as "non-existent ties") due to the addition or removal of an edge in the original directed network help predict large-magnitude changes in the synchronizability of directed networks. In particular, we demonstrated that the addition of small-world connections to a directed network surprisingly worsens its synchronizability, provided that this addition leads

to the disappearance of a large fraction of augmenting edges in the symmetrized-and-augmented network.

Based on the application of Lyapunov functions, our method gives sufficient stability conditions though it might not always predict the precise, and often complex, dependence of the coupling synchronization threshold on all possible modifications of a directed network. However, it provides a robust and direct characterization of this dependence on the mean degree imbalance controlling the "non-existent ties." Being an extension of the generalized connection method,[24] our method usually out-performs the latter in sparse and multi-component networks, where the addition of augmenting edges between distant or poorly connected nodes has a stronger impact on reducing the stability bound. With the help of the developed optimization algorithm aimed to evenly distribute traffic loads on the edges and avoid bottlenecks, our method often approaches the optimal performance of the eigenvalue-based methods in dense networks, where the choice of possible paths is abundant.

A combination of our method with the multilayer connection graph method[52] for predicting the stability of synchronization in undirected networks with multiple layers of coupling promises to become a fundamental tool for studying synchronization in directed multilayer networks, which otherwise cannot be effectively handled by the eigenvalue-based methods. This is due to the fact that the connectivity matrices corresponding to two or more connection layers do not commute in general, and, therefore, the eigenvalues of the connectivity matrices cannot be directly used. The multilayer networks are known to exhibit striking, counterintuitive effects when the replacement of a lightly loaded edge in one layer with a coupling from another layer improves the synchronization, but a similar replacement of a highly loaded edge can make the network unsynchronizable.[52] The richness of synchronization behavior in undirected multilayer networks together with the nontrivial effects of edge addition in directed single-layer networks described in this paper call for studies of synchronization in directed multilayer networks and represent a subject of future work.

APPENDIX A: THE PROOF OF THEOREM 1

In this appendix, we develop the augmented connection graph method and prove Theorem 1. Our goal is to derive upper bounds on the coupling strength that guarantees global asymptotic stability of the synchronization manifold S in the system (1). To develop our stability method, we follow the steps of the proof of the generalized connection graph method,[24] up to a certain step where we introduce a new stability argument via the addition of augmenting edges.

We introduce the difference variables

$$\mathbf{X}_{ij} = \mathbf{x}_j - \mathbf{x}_i, \quad i,j = 1,\ldots,n, \tag{A1}$$

whose global convergence to zero will imply the transversal global stability of the synchronization manifold S. Then, we subtract the ith equation from the jth equation in network system (1) to obtain the equations for the transversal stability of S

$$\dot{\mathbf{X}}_{ij} = \mathbf{F}(\mathbf{x}_j) - \mathbf{F}(\mathbf{x}_i) + d\sum_{k=1}^{n}\{w_{jk}P\mathbf{X}_{jk} - w_{ik}P\mathbf{X}_{ik}\}, \quad i,j = 1,\ldots,n. \tag{A2}$$

The function difference $\mathbf{F}(\mathbf{x}_j) - \mathbf{F}(\mathbf{x}_i)$ can be rewritten in a compact vector form

$$\mathbf{F}(\mathbf{x}_j) - \mathbf{F}(\mathbf{x}_i) = \left[\int_0^1 D\mathbf{F}(v\mathbf{x}_j + (1-v)\mathbf{x}_i)dv\right]\mathbf{X}_{ij},$$

where $D\mathbf{F}$ is the $h \times h$ Jacobian matrix of $\mathbf{F}$. Therefore, we obtain

$$\dot{\mathbf{X}}_{ij} = \left[\int_0^1 D\mathbf{F}(\beta x_j + (1-v)x_i)dv\right]X_{ij} + d\sum_{k=1}^{n}\{w_{jk}P\mathbf{X}_{jk} - w_{ik}P\mathbf{X}_{ik}\}, \quad i,j = 1,\ldots,n. \tag{A3}$$

We will prove global stability of complete synchronization in the network (1) by showing that the equilibrium $O = \{\mathbf{X}_{ij} = 0, i,j = 1,\ldots,n\}$ can be made globally asymptotically stable by increasing the coupling strength. The first intrinsic term in Eq. (A3) yields instability via the divergence of trajectories within the individual, possibly chaotic oscillators. The second term $d\sum_{k=1}^{n}\{w_{jk}P\mathbf{X}_{jk} - w_{ik}P\mathbf{X}_{ik}\}$ accounts for the contribution of the directed network connections and may overcome the unstable term, provided that the coupling is strong enough.

As in the derivation of the generalized connection graph method,[24] the difference variable system (A3) is redundant and contains all possible $(n-1)n/2$ non-zero differences $\mathbf{X}_{ij}$. Technically, only $n-1$ linearly independent differences are necessary to prove the convergence between n variables $\mathbf{X}_{ij}$. However, the consideration of all non-zero $\mathbf{X}_{ij}$ are a key component of our method, which allows cross terms to disappear in the stability description which follows.

We add and subtract additional terms $aP\mathbf{X}_{ij}$ from the difference system (A3) and obtain

$$\dot{\mathbf{X}}_{ij} = \left[\int_0^1 D\mathbf{F}(v\mathbf{x}_j + (1-v)\mathbf{x}_i)dv - aP\right]\mathbf{X}_{ij} + aP\mathbf{X}_{ij} + d\sum_{k=1}^{n}\{w_{jk}P\mathbf{X}_{jk} - w_{ik}P\mathbf{X}_{ik}\}, \quad i,j = 1,\ldots,n, \tag{A4}$$

where the positive parameter a is to be determined.

The introduction of the terms $aP\mathbf{X}_{ij}$ allows for deriving stability conditions of fixed point $\mathbf{X}_{ij} = 0$, $i,j = 1,\ldots,n$ in two steps. Notice that the negative terms $-aP\mathbf{X}_{ij}$ promote the stability of the fixed point such that increasing parameter a can help overcome instabilities caused by positive eigenvalues of the Jacobian $D\mathbf{F}$. At the same time, the instability induced by the positive terms $+aP\mathbf{X}_{ij}$ can be compensated by the coupling terms via increasing d.

We first introduce the following auxiliary systems for $i,j = 1,\ldots,n$ obtained by removing $+aP\mathbf{X}_{ij}$ and the coupling terms from system (A4)

$$\dot{\mathbf{X}}_{ij} = \left[\int_0^1 D\mathbf{F}(v\mathbf{x}_j + (1-v)\mathbf{x}_i)\,dv - aP\right]\mathbf{X}_{ij}. \tag{A5}$$

Notice that system (A5) coincides with the difference system for global stability of synchronization in a two-oscillator directed network (1) with $w_{12} > 0$ and $w_{21} = 0$

$$\dot{\mathbf{X}}_{12} = \left[\int_0^1 D\mathbf{F}(v\mathbf{x}_2 + (1-v)\mathbf{x}_1)\, dv - w_{12}dP\right]\mathbf{X}_{12}, \tag{A6}$$

where $w_{12}d$ represents the parameter a.

Our immediate goal is to place an upper bound on the value of $w_{12}d = a$ which makes the trivial fixed point $\mathbf{X}_{12} = 0$ of system (A6) globally stable and, therefore, guarantees global stability of synchronization in the simplest two-oscillator directed network (1). This also places a constraint on the choice of the individual oscillator as only Type I oscillators[5] are capable of synchronizing globally and maintaining synchronization for any coupling strength exceeding the critical threshold a. As a result, our proof is limited to Type I oscillators. The derivation of this upper bound involves the construction of a Lyapunov function $W = \frac{1}{2}\mathbf{X}_{12}^T \cdot I_h \cdot \mathbf{X}_{12}$, where I_h is an $h \times h$ identity matrix and proving that its derivative along the solutions of system (A6) is negative definite, provided that $w_{12}d > a$. This is a fairly straightforward calculation for Type I oscillators that was performed, for example, for x-coupled Lorenz oscillators in Ref. 23 and for coupled Hindmarsh–Rose neuron models in Ref. 27, where the synchronization threshold a for a two-node network was explicitly connected with the individual oscillators' parameters [see the bound (7) for two coupled Lorenz systems (6)].

Using this bound a, which guarantees the stability of the auxiliary systems (A5), we can reduce the stability analysis of the full system (A4) to the following system by eliminating the term in brackets so that

$$\dot{\mathbf{X}}_{ij} = aP\mathbf{X}_{ij} + d\sum_{k=1}^{n}\{w_{jk}P\mathbf{X}_{jk} - w_{ik}P\mathbf{X}_{ik}\}, \tag{A7}$$

where the positive term $aP\mathbf{X}_{ij}$, controlled by the bound a, promotes instability and must be compensated for by the coupling term.

We introduce a Lyapunov function

$$V = \frac{1}{4}\sum_{i=1}^{n}\sum_{j=1}^{n}\mathbf{X}_{ij}^T \cdot I_h \cdot \mathbf{X}_{ij}, \tag{A8}$$

whose time derivative along trajectories of system (A7) is

$$\dot{V} = \frac{1}{2}\sum_{i=1}^{n}\sum_{j=1}^{n} a\mathbf{X}_{ij}^T P\mathbf{X}_{ij} - \frac{1}{2}\sum_{i=1}^{n}\sum_{j=1}^{n}\sum_{k=1}^{n} d\{w_{jk}\mathbf{X}_{ji}^T P\mathbf{X}_{jk} + w_{ik}\mathbf{X}_{ik}^T P\mathbf{X}_{ij}\}. \tag{A9}$$

Performing simple algebraic manipulations (see Ref. 70 for the details of this passage), we can bound the right-hand side (RHS) of (A9) as follows:

$$\dot{V} \le \sum_{i=1}^{n-1}\sum_{j>i}^{n} a\mathbf{X}_{ij}^T P\mathbf{X}_{ij} - nd\sum_{i=1}^{n-1}\sum_{j>i}^{n}\frac{w_{ij}+w_{ji}}{2}\mathbf{X}_{ij}^T P\mathbf{X}_{ij} + \sum_{i=1}^{n-1}\sum_{j>i}^{n}\frac{D_i^b + D_j^b}{2}\mathbf{X}_{ij}^T P\mathbf{X}_{ij}, \tag{A10}$$

where $D_i^b = \sum_{k=1}^{n} w_{ki}d$ and $D_j^c = \sum_{k=1}^{n} w_{kj}d$ are the ith and jth column sums of the connection matrix D, respectively. In terms of graph quantities, the column sum $D_i^b = \sum_{k\neq i} w_{ki}d - \sum_{k\neq i} w_{ik}d$ amounts to the difference between the sums of the coupling weights of all its outgoing edges (the out-degree of node i) and of all its incoming edges (the in-degree). We call this quantity the degree imbalance of node i. The quantity $\frac{D_i^b + D_j^b}{2} = D_{ij}^b$ is then the mean degree imbalance for a pair of nodes i and j.

The negative definiteness of $\dot{V}$ implies the stability of the difference system (A4). Therefore, we need to find the conditions under which the RHS of inequality (A10) is a negative quadratic form. This yields the following inequality:

$$\sum_{v=1}^{s}\sum_{j=1,i>i}^{n}\frac{w_{ij}+w_{ji}}{2}dX_{ij}^{v\,2} - \sum_{v=1}^{s}\sum_{j=1,i>i}^{n}\frac{d}{n}D_{ij}^b X_{ij}^{v\,2} > \frac{a}{n}\sum_{v=1}^{s}\sum_{j=1,i>i}^{n} X_{ij}^{v\,2}, \tag{A11}$$

where we have replaced the vector terms $\mathbf{X}_{ij}^T P\mathbf{X}_{ij}$ with their scalar components $X_{ij}^{v\,2} = (x_j^v - x_i^v)^2$, $v = 1, \ldots, s$ (recall that the $h \times h$ projection matrix P couples the oscillators through their s first variables).

In (A11), the coupling weights $\frac{w_{ij}+w_{ji}}{2}$ correspond to edges on the symmetrized connection graph obtained by replacing a direct edge from node i to node j and an edge in the reverse direction by an undirected edge with the mean coupling weight. Therefore, the difference variables X_{ij} in the first sum on the left-hand side (LHS) of (A11) correspond to pairs of nodes directly connected by an edge on the symmetrized graph. At the same time, the difference variables in the second sum on the LHS and the sum on RHS correspond to any possible pairs of nodes. Notice that the mean degree imbalance D_{ij}^b between nodes i and j may be positive, negative, or zero. Therefore, pairs of nodes with negative D_{ij}^b yield positive terms in the second sum on LHS and are favorable for lowering inequality (A11). On the contrary, negative terms $dD_{ij}^b X_{ij}^{v\,2}$ with $D_{ij}^b > 0$ worsen inequality (A11) and should be assigned to the RHS.

So far, we have closely followed the steps of the derivation of the generalized connection graph method,[24] in which one assigns each negative term $\frac{d}{n}D_{ij}^b X_{ij}^{v\,2}$ with $D_{ij}^b > 0$ to the RHS if nodes i and j are not directly connected by an edge on the directed graph $\mathbf{D}$. As a result, the remaining positive terms $\frac{d}{n}D_{ij}^b X_{ij}^{v\,2}$ with $D_{ij}^b < 0$, where i and j are linked by an edge on $\mathbf{D}$ are left on the LHS and combined with the terms $\frac{w_{ij}+w_{ji}}{2}dX_{ij}^{v\,2}$. This amounts to weighing the symmetrized connection graph by adding an extra coupling $|\frac{d}{n}D_{ij}^b|$ to the existing symmetrized edge with coupling $\frac{w_{ij}+w_{ji}}{2}d$.

While this redistribution of the positive and negative terms $\frac{d}{n}D_{ij}^b X_{ij}^{v\,2}$ preserves the structure of the symmetrized graph and makes the application of the generalized connection graph method[24] convenient, assigning the positive terms with $D_{ij}^b < 0$ differently can be of help for improving the synchronization criterion in certain classes of directed networks, as shown in Sec. V. Here, we take this

route, which leads to our augmented graph stability method. Thus, in contrast to the generalized connection graph method, we keep all terms $dD_{ij}^b X_{ij}^{v\,2}$ with $D_{ij}^b < 0$ on the LHS of (A11). This amounts to symmetrizing and weighing the original directed connection graph **D** and adding a new undirected edge between nodes i and j if their mean degree imbalance $D_{ij}^b < 0$ and the nodes are not directly connected via the original directed graph. Therefore, to each edge k on the symmetrized-and-augmented connection graph **C**, we assign the following coupling weight:

$$c_k = \begin{cases} c_k^{sym} \text{ for existing edge } k \text{ with } D_{ij}^b \geq 0, \\ c_k^{sym} + c_k^{aug} \text{ for existing edge } k \text{ with } D_{ij}^b < 0, \\ c_k^{aug} = \left| \dfrac{D_{ij}^b}{n} \right| \text{ for augmenting edge } k, \text{ where} \end{cases} \tag{A12}$$

$$c_k^{sym} = \frac{w_{ij} + w_{ji}}{2} d, \quad c_k^{aug} = \left| \frac{D_{ij}^b}{n} \right| = \left| \frac{D_i^b + D_j^b}{2n} \right|.$$

Denote the difference variables X_{ij}^v on the LHS of (A11) by X_k^v, where $k = 1, \ldots, m$ indicates an edge on the symmetrized-and-augmented graph **C**. Notice that the graph **C** may contain more edges than the original directed graph **D**, due to the presence of augmenting edges. Thus, in terms of the undirected connection graph **C**, inequality (A11) can be re-written as follows:

$$\sum_{v=1}^{s} \sum_{k=1}^{m} c_k X_k^{v\,2} > \frac{a}{n} \sum_{v=1}^{s} \sum_{j=1, i>i}^{n} \left(1 + \chi \left(\frac{D_{ij}^b}{2a} \right) \right) X_{ij}^{v\,2}, \tag{A13}$$

where the function $\chi(\xi) = \begin{cases} \xi, & \text{if } \xi > 0 \\ 0, & \text{if } x \leq 0 \end{cases}$ indicates that only terms $\frac{D_{ij}^b}{2a} > 0$ are taken into account on the RHS. As in the connection graph method for undirected networks,[23] we seek to express all difference variables X_{ij}^v, $i, j = 1, \ldots, n$ on the RHS of (A13) through the difference variables X_k^v on the LHS that correspond to edges of the symmetrized-and-augmented graph **C**. This can be done by choosing a path from node i to node j for any pair of oscillators (i, j). We denote this path by P_{ij}. Its path length $|P_{ij}|$ is the number of edges comprising the path. For example, if the path P_{14} passes through nodes with indices 1, 2, 3, and 4, then the difference variables can be written as $X_{14}^v = x_4^v - x_1^v = (x_4^v - x_3^v) + (x_3^v - x_2^v) + (x_2^v - x_1^v) = X_{12}^v + X_{23}^v + X_{34}^v$, where the differences X_{12}^v, X_{23}^v, and X_{34}^v correspond to the edges and the path length $|P_{14}| = 3$. As we have to deal not with the variables X_{ij}^v, but with their squares $X_{ij}^{v\,2}$, we apply the Cauchy–Schwartz inequality, which yields in the above example: $X_{14}^{v\,2} = (X_{12}^v + X_{23}^v + X_{34}^v)^2 \leq 3(X_{12}^{v\,2} + X_{23}^{v\,2} + X_{34}^{v\,2})$, where the factor 3 indicates the number of edges comprising the path.

Depending on the sign of mean degree imbalance D_{ij}^b, some of the path lengths will be weighted due to the presence of nonunit factors $\left(1 + \frac{D_i^c + D_j^c}{2a} \right)$ on the RHS of inequality (A13). Thus, for any pair of nodes i and j, we associate to each chosen path P_{ij} its weighted length

$$L(P_{ij}) = \begin{cases} |P_{ij}| = 1 & \text{if } D_{ij}^b < 0, \\ \left(1 + \frac{D_{ij}^b}{a} \right) P_{ij} & \text{otherwise.} \end{cases} \tag{A14}$$

Note that a pair of nodes i and j with the mean degree imbalance $D_{ij}^b < 0$ is always connected by either an augmenting edge k with coupling strength c_k^{aug} or by a weighted combination of the augmenting edge and a symmetrized edge with the total strength $c_k^{sym} + c_k^{aug}$. As a result, the corresponding weighted path length $L(P_{ij})$ simply equals $|P_{ij}| = 1$.

Replacing the square terms $X_{ij}^{v\,2}$ on the RHS with their bounds expressed via $X_k^{v\,2}$ and collecting the weighted path lengths $L(P_{ij})$, we can turn inequality (A13) into the following condition:

$$\sum_{v=1}^{s} \sum_{k=1}^{m} c_k X_k^{v\,2} > \frac{a}{n} \sum_{v=1}^{s} \sum_{k=1}^{m} b_k X_k^{v\,2}, \tag{A15}$$

where $b_k = \sum_{j>i;\, k \in P_{ij}}^{n} L(P_{ij})$ is the total weighted length of the chosen paths P_{ij} that go through a given edge k on the symmetrized-and-augmented graph **C**. Dropping the summation signs and the difference variables, we obtain the criterion on the coupling strengths of each edge of the symmetrized-and-augmented graph **C**, which guarantees positive definiteness of the time derivative $\dot{V}$,

$$c_k > \frac{a}{n} b_k, \quad k = 1, \ldots, m. \tag{A16}$$

Therefore, under condition (A16), complete synchronization in the original directed network (1) is globally asymptotically stable. This completes the proof of Theorem 1.

APPENDIX B: THE OPTIMIZATION ALGORITHM

The optimization algorithm for choosing paths that minimize the synchronization bound (5) is as follows:

- *Step A*: Allocate an indexable queue Q of path choices where each entry of Q contains a choice of a path from every node to every other node. Initialize Q with a single element containing the set of one shortest path between each node pair. Denote by Q_0 the first entry of Q at the current iteration, that is, the next choice of paths to consider, being the least recently inserted entry. Consider a set V of elements, which have been removed from Q; initially, V is the empty set. Let $d^\star$ be the current best bound on the synchronization threshold determined by the algorithm. Initially, $d^\star = \infty$.
- *Step B*: Compute the synchronization bound (5), $d_{new}^\star$, for the symmetrized-and-augmented network, using the choice of paths Q_0. Identify the bottleneck edge e_{uv}, which yields the synchronization bound. Pick a chosen path P_{ij} between two nodes i, j that traverses the bottleneck edge and reroute the path through a different vertex adjacent to u. Replace P_{ij} with the rerouted path in Q_0 and store the resulting set of paths in a new variable Q_1.
- *Step C*: If, and only if, $d_{new}^\star < d^\star$, reset $d^\star = d_{new}^\star$, and if $Q_1 \notin V$, insert Q_1 into Q and V.
- *Step D*: Repeat steps B and C until Q is empty.
- *Step E*: When the procedure terminates, $d^\star$ is the lowest bound on the synchronization threshold obtainable by this algorithm.

Figure 6 presents a simple example of a dense network for which our optimization algorithm significantly improves the synchronization bound d^*. The use of the shortest path between each

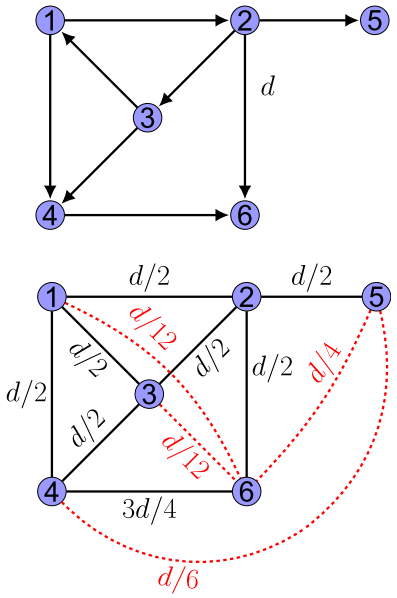

FIG. 6. An example of a network for which the optimization algorithm significantly lowers the bound (A13), from $d^\star = 10a$ to $d^\star = 2a$. The eigenvalue-based bound is $\frac{a}{|\Re\lambda_2|} = a$. (Top): Directed network with uniform coupling strength d. (Bottom): Corresponding symmetrized-and-augmented graph with four augmenting edges (red dotted lines).

node pair to calculate traffic load b_k in (5) yields a conservative upper bound on the synchronization threshold: $d_{12}^* = 10a$ due to the long path $P_{24} = e_{21}, e_{14}$ through the bottleneck edge e_{12} in the symmetrized-and-augmented graph [Fig. 6 (bottom)]. Our algorithm then attempts to reroute each chosen path which goes through the bottleneck edge e_{12}. The rerouting of path P_{24} through edges e_{26} and e_{64} yields the inequality $d_{12}^* > 2a$ on the bottleneck edge without producing a worse bound on any other edge. Therefore, the bound is reduced significantly, i.e., by a factor of 5, due to reduced traffic load on edge e_{12}. Further re-routings do not yield improvements on this bound. Therefore, the procedure terminates after seven iterations. Further details of the above calculations can be found in a Python implementation of the optimization algorithm applied to this network.[59]

ACKNOWLEDGMENTS

This work was supported by the National Science Foundation (NSF) (USA) under Grant Nos. DMS-1909924 and DMS-1616345 (to K.D. and I.V.B.). and the Ministry of Science and Higher Education of the Russian Federation (project No. 0729-2020-0036) (to I.V.B.). K.Z. contributed to this article in his personal capacity. The views expressed are his own and do not necessarily represent the views of the Centers for Disease and Control and Prevention or the U.S. Government.

REFERENCES

[1] M. S. Granovetter, in *Social Networks* (Elsevier, 1977), pp. 347–367.
[2] S. H. Strogatz, Nature **410**, 268 (2001).
[3] M. E. Newman, SIAM Rev. **45**, 167 (2003).
[4] A. Pikovsky, M. Rosenblum, and J. Kurths, *Synchronization: A Universal Concept in Nonlinear Sciences* (Cambridge University Press, 2003), Vol. 12.
[5] S. Boccaletti, V. Latora, Y. Moreno, M. Chavez, and D.-U. Hwang, Phys. Rep. **424**, 175 (2006).
[6] J. A. Wolf and P. F. Koch, Front Syst. Neurosci. **10**, 43 (2016).
[7] K. Schindler, C. E. Elger, and K. Lehnertz, Clin. Neurophysiol. **118**, 1955 (2007).
[8] C. Hammond, H. Bergman, and P. Brown, Trends Neurosci. **30**, 357 (2007).
[9] A. E. Motter, S. A. Myers, M. Anghel, and T. Nishikawa, Nat. Phys. **9**, 191 (2013).
[10] S. Camazine, J.-L. Deneubourg, N. R. Franks, J. Sneyd, E. Bonabeau, and G. Theraulaz, *Self-Organization in Biological Systems* (Princeton University Press, 2003), Vol. 7.
[11] S. H. Strogatz, D. M. Abrams, A. McRobie, B. Eckhardt, and E. Ott, Nature **438**, 43 (2005).
[12] I. V. Belykh, R. Jeter, and V. N. Belykh, Chaos **26**, 116314 (2016).
[13] I. Belykh, R. Jeter, and V. Belykh, Sci. Adv. **3**, e1701512 (2017).
[14] L. M. Pecora and T. L. Carroll, Phys. Rev. Lett. **80**, 2109 (1998).
[15] J. F. Heagy, L. M. Pecora, and T. L. Carroll, Phys. Rev. Lett. **74**, 4185 (1995).
[16] C. W. Wu and L. O. Chua, IEEE Trans. Circuits Syst. I Fundam. Theory Appl. **43**, 161 (1996).
[17] L. M. Pecora, Phys. Rev. E **58**, 347 (1998).
[18] S. Boccaletti, J. Kurths, G. Osipov, D. Valladares, and C. Zhou, Phys. Rep. **366**, 1 (2002).
[19] M. Barahona and L. M. Pecora, Phys. Rev. Lett. **89**, 054101 (2002).
[20] C. W. Wu, *Synchronization in Coupled Chaotic Circuits and Systems* (World Scientific, 2002), Vol. 41.
[21] A. Pogromsky and H. Nijmeijer, IEEE Trans. Circuits Syst. I Fundam. Theory Appl. **48**, 152 (2001).
[22] X. F. Wang and G. Chen, IEEE Trans. Circuits Syst. I Fundam. Theory Appl. **49**, 54 (2002).
[23] V. N. Belykh, I. V. Belykh, and M. Hasler, Physica D **195**, 159 (2004).
[24] I. Belykh, V. Belykh, and M. Hasler, Physica D **224**, 42 (2006).
[25] C. W. Wu, IEEE Trans. Automat. Contr. **51**, 1207 (2006).
[26] Z. Li and G. Chen, IEEE Trans. Circuits Syst. II Express Briefs **53**, 28 (2006).
[27] I. Belykh, M. Hasler, M. Lauret, and H. Nijmeijer, Int. J. Bifurcat. Chaos **15**, 3423 (2005).
[28] I. Belykh and A. Shilnikov, Phys. Rev. Lett. **101**, 078102 (2008).
[29] J. Sun, E. M. Bollt, and T. Nishikawa, Europhys. Lett. **85**, 60011 (2009).
[30] T. Nishikawa and A. E. Motter, Proc. Natl. Acad. Sci. U.S.A. **107**, 10342 (2010).
[31] H. Nakao, T. Yanagita, and Y. Kawamura, Phys. Rev. X **4**, 021032 (2014).
[32] J. Aguirre, R. Sevilla-Escoboza, R. Gutiérrez, D. Papo, and J. Buldú, Phys. Rev. Lett. **112**, 248701 (2014).
[33] L. Zhang, A. E. Motter, and T. Nishikawa, Phys. Rev. Lett. **118**, 174102 (2017).
[34] L. Chen, P. Ji, D. Waxman, W. Lin, and J. Kurths, Chaos **29**, 083131 (2019).
[35] T. Nishikawa, J. Sun, and A. E. Motter, Phys. Rev. X **7**, 041044 (2017).
[36] D. Taylor, P. S. Skardal, and J. Sun, SIAM J. Appl. Math. **76**, 1984 (2016).
[37] I. Belykh, V. Belykh, and M. Hasler, Physica D **195**, 188 (2004).
[38] M. Porfiri, D. J. Stilwell, E. M. Bollt, and J. D. Skufca, Physica D **224**, 102 (2006).
[39] F. Sorrentino and E. Ott, Phys. Rev. Lett. **100**, 114101 (2008).
[40] M. Chen, Y. Shang, C. Zhou, Y. Wu, and J. Kurths, Chaos **19**, 013105 (2009).
[41] M. Frasca, A. Buscarino, A. Rizzo, L. Fortuna, and S. Boccaletti, Phys. Rev. Lett. **100**, 044102 (2008).
[42] P. DeLellis, M. Di Bernardo, T. E. Gorochowski, and G. Russo, IEEE Circuits Syst. Mag. **10**, 64 (2010).
[43] R. Jeter and I. Belykh, IEEE Trans. Circuits Syst. I Reg. Pap. **62**, 1260 (2015).
[44] I. Belykh, M. di Bernardo, J. Kurths, and M. Porfiri, Physica D **267**, 1 (2014).
[45] W. Lin, X. Chen, and S. Zhou, Chaos **27**, 073110 (2017).
[46] R. Jeter, M. Porfiri, and I. Belykh, IEEE Control Syst. Lett. **2**, 103 (2017).
[47] R. Jeter, M. Porfiri, and I. Belykh, Chaos **28**, 071104 (2018).
[48] F. Sorrentino, New J. Phys. **14**, 033035 (2012).
[49] D. Irving and F. Sorrentino, Phys. Rev. E **86**, 056102 (2012).
[50] C. I. del Genio, J. Gómez-Gardeñes, I. Bonamassa, and S. Boccaletti, Sci. Adv. **2**, e1601679 (2016).

[51]X. Zhang, S. Boccaletti, S. Guan, and Z. Liu, Phys. Rev. Lett. **114**, 038701 (2015).
[52]I. Belykh, D. Carter, and R. Jeter, SIAM J. Appl. Dyn. Syst. **18**(4), 2267–2302 (2019).
[53]T. Nishikawa and A. E. Motter, Phys. Rev. Lett. **117**, 114101 (2016).
[54]I. Belykh, R. Reimbayev, and K. Zhao, Phys. Rev. E **91**, 062919 (2015).
[55]R. Reimbayev, K. Daley, and I. Belykh, Philos. Trans. R. Soc. A **375**, 20160282 (2017).
[56]K. S. Fink, G. Johnson, T. Carroll, D. Mar, and L. Pecora, Phys. Rev. E **61**, 5080 (2000).
[57]C. W. Wu, Int. J. Bifurcat. Chaos **12**, 2233 (2002).
[58]C. Poignard, J. P. Pade, and T. Pereira, J. Nonlinear Sci. **29**, 1919 (2019).
[59]Python implementation of the augmented graph method with and without optimization applied to the network of Fig. 6 is available online at https://github.com/KevinMichaelDaley/nonexistent_ties.
[60]M. Fiedler, Czechoslovak Math. J. **23**, 298 (1973).
[61]E. N. Lorenz, J. Atmosp. Sci. **20**, 130 (1963).
[62]R. N. Madan, *Chua's Circuit: A Paradigm for Chaos* (World Scientific Publishing, 1993).
[63]O. E. Rössler, Phys. Lett. A **57**, 397 (1976).
[64]M. L. Rosenzweig and R. H. MacArthur, Am. Nat. **97**, 209 (1963).
[65]I. Belykh, C. Piccardi, and S. Rinaldi, J. Biol. Dyn. **3**, 497 (2009).
[66]V. N. Belykh, N. N. Verichev, L. Kocarev, and L. Chua, J. Circuits Syst. Comput. **3**, 579 (1993).
[67]I. Belykh, M. Hasler, and V. Belykh, Int. J. Bifurcat. Chaos **17**, 3387 (2007).
[68]R. Jeter and I. Belykh, Int. J. Bifurcat. Chaos **25**, 1540002 (2015).
[69]I. Belykh, V. Belykh, K. Nevidin, and M. Hasler, Chaos **13**, 165 (2003).
[70]I. Belykh, V. Belykh, and M. Hasler, Chaos **16**, 015102 (2006).